188

JOURNAL OF APPLIED PHYSICS VOLUME 84, NUMBER 5 1 SEPTEMBER 1998

Shear localization and chemical reaction in Ti–Si and Nb–Si powder mixtures: Thermochemical analysis

H. C. Chen, V. F. Nesterenko, and M. A. Meyers
Department of Applied Mechanics and Engineering Sciences, University of California, San Diego, La Jolla, California 92093

(Received 17 June 1997; accepted for publication 3 June 1998)

Chemical reactions in Ti–Si and Nb–Si powder mixtures were initiated in regions of high plastic strain induced by high-strain-rate deformation. These regions of high localized plastic strain had thicknesses of 10–25 μm and a characteristic spacing of 600–1000 μm. Scaling up of the experiments revealed a shear-band spacing that is constant and dictated by material and deformation parameters. The generation of heat due to plastic deformation and chemical reaction is treated in a one-dimensional calculation. The calculations are in qualitative agreement with experimental results: shear bands can serve as ignition regions for the propagation of the reaction throughout the entire specimen for Ti–Si, whereas in the Nb–Si system (that has a much lower enthalpy of reaction), the reaction is always localized in the shear bands. These results enable the estimation of a reaction time in the Ti–Si mixture (~10 ms) and of a critical global strain required for the complete reaction to take place (ϵ_{eff}=0.38). This is a new regime of reaction, intermediate between combustion synthesis and shock compression synthesis. © *1998 American Institute of Physics.* [S0021-8979(98)08117-1]

I. INTRODUCTION

The synthesis of materials by the propagation of a combustion wave is an area of research that has been receiving a great deal of attention;[1–4] the pioneering work by Merzhanov, Borovinskaya, and co-workers,[5,6] starting in 1965, has identified and characterized combustion reactions in a large number of powder mixtures. This process involves ignition (either by an external source or by preheating the sample), generating a self-propagation combustion wave which synthesizes the compound from the reactants through an exothermic reaction. In parallel and related research, exothermic chemical reactions initiated by shock compression were reported by Kimura[7] in 1963; extensive investigations in the past 30 years identified a large number of shock-induced reactions.[8–11]

It has recently been observed that plastic deformation without shock-wave loading can initiate chemical reactions in powder mixtures.[12–14] This occurs in regions of high localized plastic strain and under high-strain-rate deformation which ensures adiabatic or quasi-adiabatic conditions in the narrow deformation bands. This regime is intermediary between thermal combustion synthesis and shock-induced reactions. The associated temperature rise and mechanical flow of constituents are sufficient to initiate the chemical reaction within these regions. The objectives of the research whose results are reported herein are:

(a) to establish the critical conditions for initiation and propagation of reactions in two systems with widely varying heats of reaction: Nb–Si ($\Delta H=-138$ kJ/mole) and Ti–Si (−580 kJ/mole);
(b) to model the initiation of reaction and its propagation throughout the inter-shear-band regions and to explain the difference between the response of the two systems.

II. EXPERIMENTAL TECHNIQUE

Ti–Si (74 wt %–26 wt %) and Nb–Si (68 wt %–32 wt %) powder mixtures in their stoichiometric compositions of intermetallic compounds, Ti_5Si_3 and $NbSi_2$, respectively, were used in this research. The powders (from CERAC) had sizes of −325 mesh (<44 μm), high purity (>99.5%), and irregular shape. These compounds had been investigated in earlier shock experiments[15] and are therefore well characterized. These systems have quite different enthalpies of reaction, ΔH:[16]

$$5\ Ti+3\ Si \rightarrow Ti_5Si_3 \quad \Delta H=-580\ \text{kJ/mole},$$

$$Nb+2\ Si \rightarrow NbSi_2 \quad \Delta H=-138\ \text{kJ/mole}.$$

These differences in heat of reaction can result in widely different sensitivities to the initiation and propagation of reaction. Yu[17] and Meyers *et al.*[16] calculated shock threshold pressures for reaction at 65% initial density and obtained values of 1.5 and 9 GPa for Ti_5Si_3 and $NbSi_2$, respectively. These calculations are based on the Krueger–Vreeland criterion[18] and are consistent with experimental results of Yu[15] and Vecchio *et al.*[19]

The thick-walled cylinder method was developed by Nesterenko *et al.*[20,21] for the investigation of high-strain, high-strain rate deformation of solid materials (metals, ceramics and polymers), and modified for the study of inert and reactive porous powder mixtures.[12,14] The schematic of the setup is shown in Fig. 1. Detonation is initiated at the top of the charge and propagates along the cylinder axis. The powder is first consolidated by a low detonation velocity explosive charge, which produces weak shock loading with pressures less than 1 GPa and without any chemical reactions [Fig. 1(a)]. An orifice is then drilled along the cylinder axis and a second explosive event is carried out [Fig. 1(b)]. This

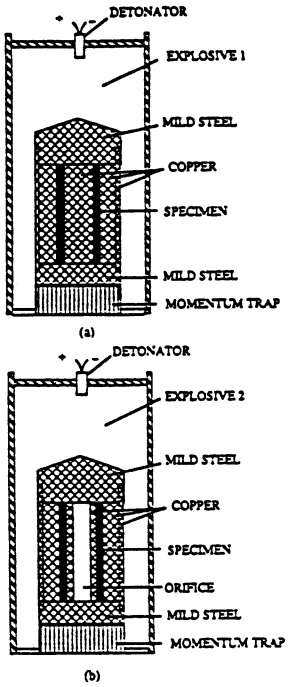

FIG. 1. Schematic of setup for thick-walled cylinder (TWC): (a) first (consolidation) explosive event, (b) second (deformation) explosive event.

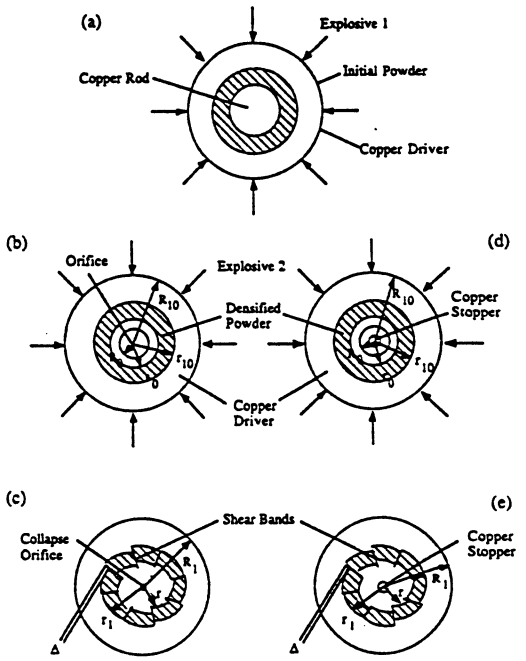

FIG. 2. Geometry and sequence of deformation events in thick-walled cylinder method: (a) initial geometry, densified by explosive 1; (b) densified powder with central orifice cylinder collapsed by explosive 2; (c) final geometry; (d) densified powder with copper stopper; (e) final geometry.

second explosive produces significant plastic deformation in the densified powder layer. The velocity of the inner cylinder surface and the collapse time were measured by a noncontact electromagnetic method.[20]

The sequence of events leading to densification, and controlled and prescribed shear localization in the samples, is shown in the top-view sketches in Fig. 2. A porous powder was initially placed in a tubular cavity between a central copper rod (diameter of 16 mm) and an outer copper tube (inner diameter of 20 mm and outer diameter of 31 mm). Explosive 1 [mixture of ammonite and sand in 3:1 volume ratio, Fig. 2(a)] with low detonation velocity (3.1 km/s) was used to densify the powder. No significant shear localization was observed after this stage because the global deformation is sufficiently small (final diameter of inner surface of driving copper cylinder is equal to 18–19 mm). This stage produced mainly an increase in the density of the powder by reducing its porosity. The following densifications were accomplished by the first explosive event [Fig. 2(a)]: Ti–Si mixture from ~35% to 65% of theoretical density; and Nb–Si mixture from ~50% to ~75% of theoretical density. A cylindrical hole 11 mm in diameter was drilled along the longitudinal axis of the copper rod and this composite cylinder was collapsed by the detonation of a second cylindrical explosive charge [ammonite, Fig. 2(b)] with a detonation velocity of 4.0 km/s, an initial density of 1 g/cm^3, and an outer diameter of 60 mm. This explosive event 2 produced significant plastic deformation in the densified porous layer which was highly localized in shear bands and not homogeneously distributed [Fig. 2(c)]. To prescribe the global strains, a cylindrical copper rod was inserted into the central orifice after explosive event 1 [Fig. 2(d)]. The variation of this rod diameter provides the critical initiation and propagation conditions for shear localization and chemical reaction. The explosive event 2 was also conducted on the Ti–Si mixtures without creating a central orifice. After this shock loading (without collapse) process, no shear localization or chemical reaction was observed. This confirms in the present experiments that the chemical reactions are truly strain controlled and that shock compression did not play a role; the shock pressure was purposedly kept below the threshold for shock initiation.

For the Nb–Si mixture, two scales of experiment were used, with application of the procedure described above (explosive events 1 and 2). The scaled-up experiment had dimensions approximately twice as large: the inner and outer diameter of the porous reactive mixture were 32 and 36 mm, respectively, before the densification stage; the diameter of the central orifice was increased to 22 mm, the outer diameter of driver was 60 mm, the explosive diameter was 120 mm, and the detonation velocity was 4.65 km/s. This larger detonation velocity (in comparison with the small-scale experiments) is due to the doubling of the explosive diameters from 60 to 120 mm; detonation velocity increases with charge diameter.

The global strain can be obtained from the strains in the incompressible copper shell driving the collapse process. The strain state in the uniformly deformed incompressible material is pure shear[22] and the deformation of an element is depicted in Fig. 3. The radial and tangential true strains (ϵ_r,

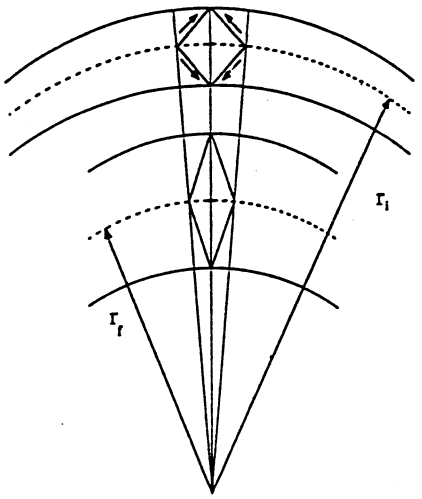

FIG. 3. Geometry of pure shear in incompressible thick-walled cylinder under uniform plastic deformation, r_i and r_f, are initial and final radii of one element.

and $\epsilon_{\varphi\varphi}$) for the copper shell, before the onset of localization, can be established from the initial and final radii, r_i and r_f, at a general point:

$$\epsilon_{rr}=-\epsilon_{\varphi\varphi}=\ln\left(\frac{r_i}{r_f}\right), \tag{1}$$

The true strains in the inner and outer surfaces of the initial porous tubular layer can be found from Eq. (1). The final radii r_f and R (or R_1) and initial radius R_0 (or R_{10}) (Fig. 2) are experimentally measured and the value of r_i, which corresponds to a preselected value of r_f, can be calculated by using conservation of mass:

$$r_i^2=r_f^2+R_0^2-R^2=r_f^2+R_{10}^2-R_1^2, \tag{2}$$

where R and R_1 are the final radii of the inner hole and outer cylinder surface. The effective strains can be calculated according to:

$$\epsilon_{\text{eff}}=\frac{\sqrt{2}}{3}\left[(\epsilon_{rr}-\epsilon_{\varphi\varphi})^2+(\epsilon_{\varphi\varphi}-\epsilon_{zz})^2+(\epsilon_{zz}-\epsilon_{rr})^2\right]^{1/2}$$

$$=\frac{2}{\sqrt{3}}\epsilon_{rr}. \tag{3}$$

The global strains in copper at the boundary with the porous layer outside the shear localization region can be estimated by using Eqs. (1) and (3) Table I shows the calculated results.

The state of stress in these plane strain experiments is very difficult to control, because during plastic flow the stresses are determined by the material strength and its dependence on temperature, strain, and strain rate. The following two main features of this method should be mentioned:

(i) The weak shock waves propagating in materials in the first stage of collapse (explosive event 1) have no noticeable influence on the chemical reaction; their amplitudes are less than 1 GPa.

(ii) The superimposed "hydrostatic" pressure inside the collapsing incompressible cylinder,[14] as a result of its acceleration toward the center, is less than 0.1 GPa.

Thus, pressure effects can be neglected to a first approximation and chemical processes are mainly strain controlled.

III. RESULTS AND DISCUSSION

Figure 4 shows the cross sections of Ti–Si (a),(b) and Nb–Si (c),(d) samples after explosive event 2. Shear localization is a prominent feature of the plastic deformation process. The shear-band spacing, L, is unaffected by the scale of experiments for the Nb–Si mixtures. The diameter in Fig. 4(d) is approximately double that of Fig. 4(c). The spacing of the shear bands for Nb–Si mixture is approximately the same as for the Ti–Si mixture: 600–1000 μm. The maximum amount of displacement, Δ, in the shear bands was higher for the large scale experiment than for the smaller scale experiment [compare Figs. 4(c) and 4(d)].

Chemical reactions are observed in the shear localization regions in both Ti–Si and Nb–Si mixtures (Fig. 5). The intense localized plastic deformation work can lead to reaction ignition inside shear band.[12–14] Under favorable circumstances, this reaction can propagate throughout the material. Since the strain rate is high, there is not sufficient time for the heat resulting from shear deformation to be conducted away from the shear localization regions. Therefore, the temperature in the shear localization regions increases to very high values. This localized temperature zone is a heat source. The shear localization regions can be treated as a one-dimensional array of "hot spots" [17] where chemical reactions are possible. Once the temperature reaches some critical value, the chemical reactions are initiated. Calculations of heat evolution for an idealized periodic distribution of "hot spots" in reactive powder mixtures were carried out. Figure 6 is a schematic illustration of the idealized model. The "hot" shear localization regions (shaded areas) have a width, δ, and a spacing, L. The temperature inside the shear localization regions increases to T_s during deformation [shown in Fig. 6(a)]. If T_s is sufficiently high, chemical reactions between components in the powder mixtures are initiated. At this time, the reaction heat, Q, is released and the temperature increases by some amount ΔT; the temperature inside the shear localization regions becomes $T_s+\Delta T$ [Fig. 6(b)]. However, the surrounding powder mixtures are at a lower temperature ($T=T_0$). The heat will be conducted to the surrounding material. The conservation of energy for this model is given by:

$$\rho C_p\frac{\partial T}{\partial t}=k\frac{\partial^2 T}{\partial x^2}+\rho Q\frac{\partial \eta}{\partial t}+\tau\frac{\partial \gamma}{\partial t}, \tag{4}$$

where ρ is the density (kg/m^3), C_p is the heat capacity (J/kg K), k is the thermal conductivity (W/m K), η is the degree of conversion, τ is the shear stress (N/m^2), γ is the shear strain, and Q is the heat of reaction. For the sake of simplicity, the following assumptions are made:

(a) The shear localization and the chemical reaction do not occur simultaneously i.e., they occur sequentially.

JOBNAME: Using JPF1 format PAGE: 4 SESS: 6 OUTPUT: Wed Jul 1 14:12:15 1998
/first/journals/jap/1sep98/081817japi
BY: innodata REV: dgalanti@jupiter/first/CLS_Journals/GRP_Jap/JOB_1sep98/DIV_081817japi ♦ 081817jap
ALINK:

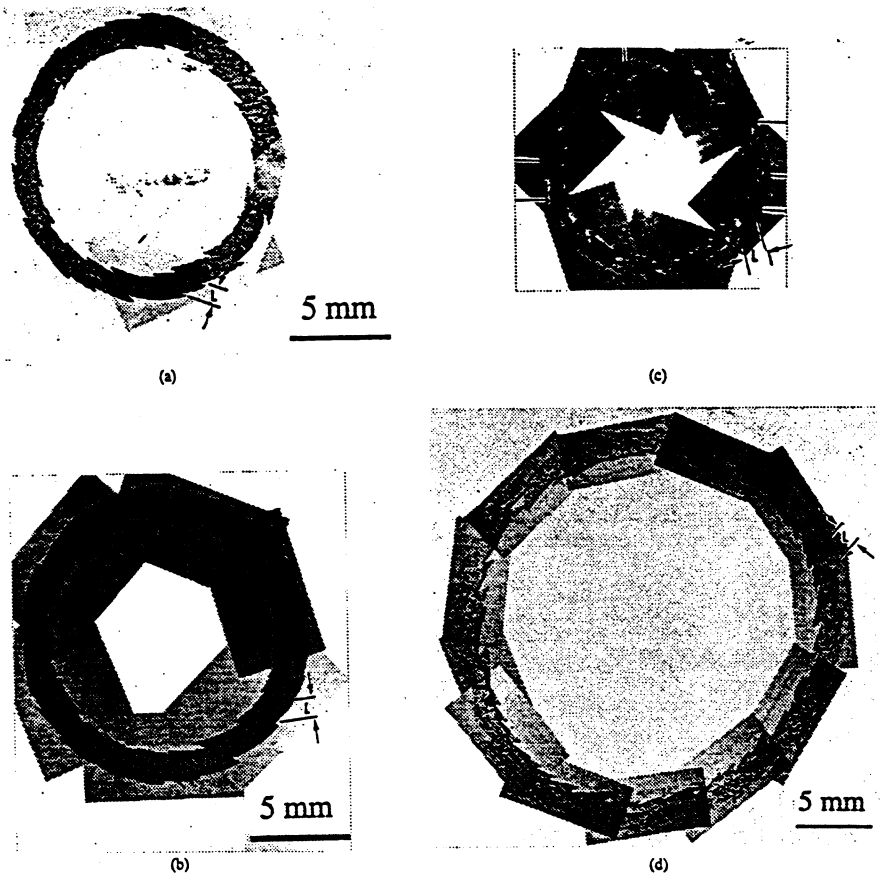

FIG. 4. Shear-band spacing at: (a) ϵ_{eff}=0.35, (b) ϵ_{eff}=0.38 in Ti–Si system, and (c) ϵ_{eff}=0.35, (d) ϵ_{eff}=0.38 in Nb–Si system.

(b) The initiation of the reaction process ($t=0$) is defined when T_s is reached. After this moment the term representing deformation work can be eliminated because at high values of T_s the drop in material strength makes this term negligible in comparison with heat release due to the reaction. Equation (4) can be rewritten as:

$$\rho C_p \frac{\partial T}{\partial t} = k \frac{\partial^2 T}{\partial x^2} + \rho Q \frac{\partial \eta}{\partial t}. \tag{5}$$

A first—order Arrhenius equation is used for reaction kinetics:

$$\frac{\partial \eta}{\partial t} = K_i (1-\eta) \exp(-E/RT). \tag{6}$$

In Eq. (6), the rate constant K_i can be greatly different inside and outside shear band. The following factors lead to an acceleration of the reaction rate inside the shear bands:

(1) The total surface of interface among particles increases with plastic strain. To a first approximation, the surface of a particle increases from $6a^2$ (for initially cubic particles with side a) to $2a^2(2+\sqrt{1+\gamma^2})$, where γ is the shear strain undergone by a particle in simple shear. Hence, the total interface, per particle, for large shear strains increases by approximately a factor equal to $(2+\gamma)/3$. This means that, after a shear strain of 30, the interfacial area (where reaction is initiated) is ten times higher.
(2) The intense localized macroshear (in shear band) creates fresh and hot surfaces as a result of localized mesoshear (inside particle[23]), friction, and removes contamination layers at the particle surfaces. These factors should enhance reactivity.
(3) Plastic deformation of particles increases their defect density. This could also be a contributory factor for acceleration of kinetics.
(4) Particle fracture, vorticity and relative motion of components can greatly intensify yield of reaction.[12,14,24]

Reaction kinetics equation [Eq. (6)] is commonly used in the combustion synthesis literature. One of the problems connected with this type of kinetics is that it theoretically provides the possibility for complete reaction at any temperature under thermal isolation. For the self-propagating mode of combustion synthesis, these kinetics allow the identification of some critical conditions like the ignition temperature. It is defined as the minimum temperature required to initiate a self-propagating reaction wave with a stationary profile under specified boundary conditions.[25] This ignition temperature is a function of the thermophysical parameters

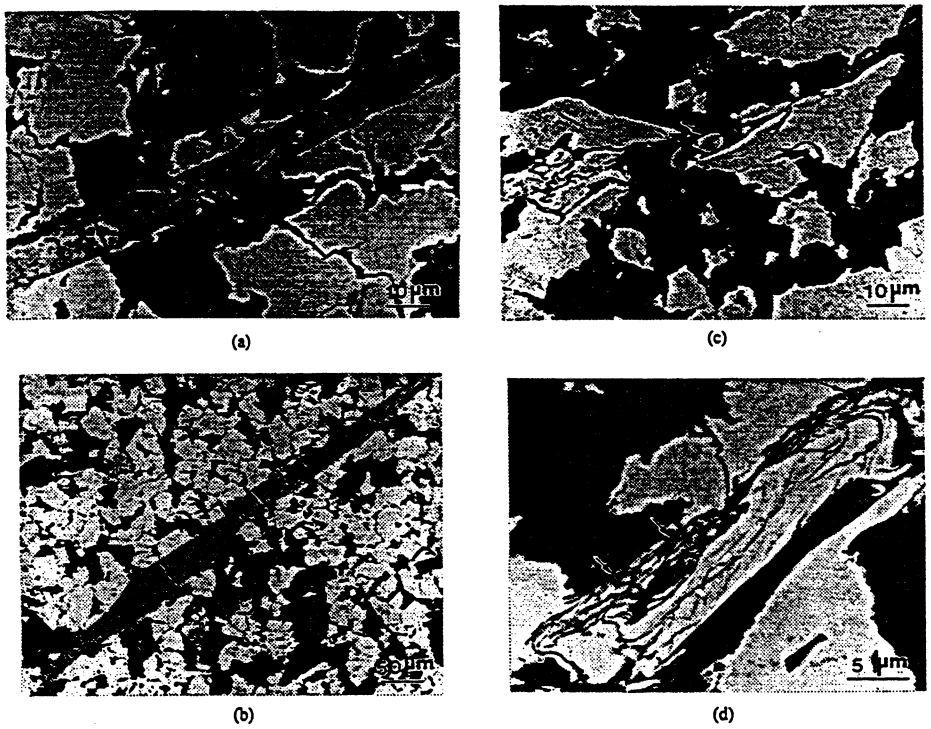

FIG. 5. The chemical reaction inside shear localization regions: (a) partial reaction ($\gamma=20$) and (b) total reaction ($\gamma=40$) in Ti–Si system; (c) and (d) partial reactions (at $\gamma=30$ and $\gamma=70$, respectively) in Nb–Si system.

of reactive material and boundary conditions. There is another case—simultaneous combustion mode of reaction—where the heating of an entire sample at a constant rate can result in bulk combustion at some critical temperature which is also called ignition temperature. This ignition temperature is also a function of material properties such as density and boundary conditions.[26] It is reasonable to equate the ignition temperature with the melting temperature of one of the components; in our case this is the melting of Si. In some cases the ignition temperature can be lower than the melting temperature of components as a result of enhanced solid state reactivity of powders after plastic deformation.[27]

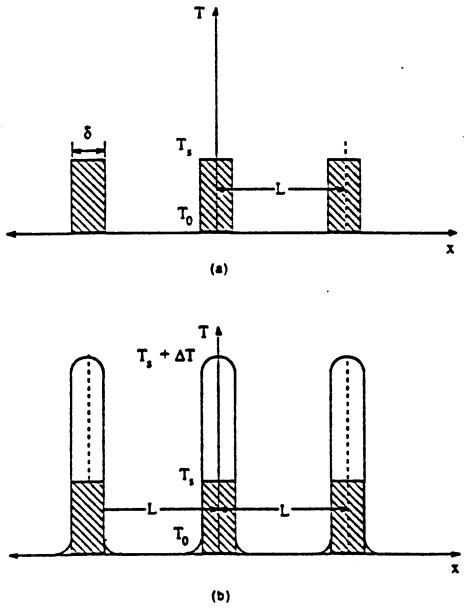

FIG. 6. Schematic one-dimensional model of periodic "hot spot": (a) temperature distribution after shear localization; (b) temperature distribution after chemical reaction initiation.

In the problem of reaction initiation by shear bands the achievement of the steady combustion wave propagation regime cannot be considered as the necessary condition. It is considered that the condition of ignition is fulfilled if the quasi-equilibrium temperature in the unit cell (after a fast stage of heat propagation from shear band and subsequent partial reaction) is close to melting temperature of Si. It is assumed that the final stage of reaction can be accomplished in the simultaneous combustion mode under natural boundary conditions provided by the contact of reactive material with copper.

The initial conditions are:

$$T(x,0)=\begin{cases} T_s & \text{at } 0\leqslant x<\delta/2, L-\delta/2<x\leqslant L \\ T_0 & \text{at } \delta/2\leqslant x\leqslant L-\delta/2 \end{cases}. \tag{7}$$

The boundary conditions represent zero heat flux at points of symmetry in the one-dimensional system of "hot" layers (Fig. 6):

$$\frac{\partial T(x,t)}{\partial x}=0 \quad \text{at} \quad x=0, L/2, L \tag{8}$$

In real experiments, the reactive mixture is encapsulated into cold copper jackets (Figs. 1 and 2) which determine macroscopic boundary conditions on the interface of reactive mixture and copper.[24] In accord with the experiments, the condition of ignition is determined as the achievement by the intermediate "equilibrium" temperature of the melting temperature of Si in the thermally isolated unit cell. Thus, if $T_{m,Si}$ is reached, the rate of subsequent reaction will be fast enough to complete reaction in the bulk, except in a thin layer adjacent to the copper. This was used by Chen *et al.*[24] to obtain the pre-exponential parameter in Eq. (6). Thermophysical properties are assumed constant and equal $\rho=3.85\times10^3$ kg/m^3, $C_p=570$ J/kg K, $k=36.5$ W/mK, $E=125$ kJ/mol and $Q=1792$ J/kg. The reaction rate outside shear band K_0 was estimated by Chen *et al.*[24] ($K_0=2.6\times10^5$ s^{-1}) and applied to estimate the temperature profile at different times. The rate constant inside shear band K_1 was selected to be equal to K_0 or $10K_0$. The increased value of $10K_0$ represents the faster reaction kinetics inside shear band (see items 1–4 above) and helps to establish whether it affects the temperature profile outside of the shear band.

The calculated temperature profiles for the Ti–Si system at $T_s\approx1350$ K ($\gamma=10$), 1685 K ($\gamma=40$), and 1750 K ($\gamma=60$),[24] are shown in Fig. 7 ($K_i=K_0$) and Fig. 8 ($K_i=10K_0$). The calculated temperature profiles can be used to predict the critical parameters for initiation and propagation of the reaction. For example, if the intermediate "equilibrium" temperature is still lower, but close to initiation temperature $T_{m,Si}$ it is probable that conditions are close to the threshold for the complete reaction in the material bulk. A slight increase of the initial temperature T_s or shear strain γ will result in complete reaction.

In both cases ($K_i=K_0$ and $K_i=10K_0$), at $T_s\approx1350$ K, heat transfer is dominant and there is no temperature increase inside the shear band as shown in Figs. 7(a) and 8(a) due to the absence of chemical reaction [Eq. (6)]. At $T_s\approx1685$ K, the temperature increases inside the shear band due to the heat release of chemical reaction. However, the reaction cannot propagate because of the low reaction rate due to the relatively low initial temperature [Figs. 7(b) and 8(b)]. Reaction is quenched at a distance 75 μm ($K_i=K_0$) and 90 μm ($K_i=10K_0$) from the center of the shear band. "Equilibrium" temperatures in these cases are about 1000 and 1100 K, respectively, and they are less than the melting temperature of Si. The increase of rate constant inside the shear band resulted in slightly higher maximum temperature in the center of the shear band (3100 and 3700 K) and in some increase of reacted zone (where $T\geqslant T_{m,Si}$).

When the temperature T_s at the initial moment ($t=0$) reaches 1750 K, the reaction rate is higher than at $T_s\approx1685$ K. Therefore, the heat can be sustained inside the shear band and the temperature experiences a dramatic increase. After reaction completion inside the shear band, the temperature there begins to decrease and the temperature outside the shear band increases due to heat conduction. As the temperature at a generic point outside the shear band reaches a critical value $T_{m,Si}$ the reaction is initiated. The reaction eventually propagates through the entire specimen. The advance of the reaction is shown in the calculations. The

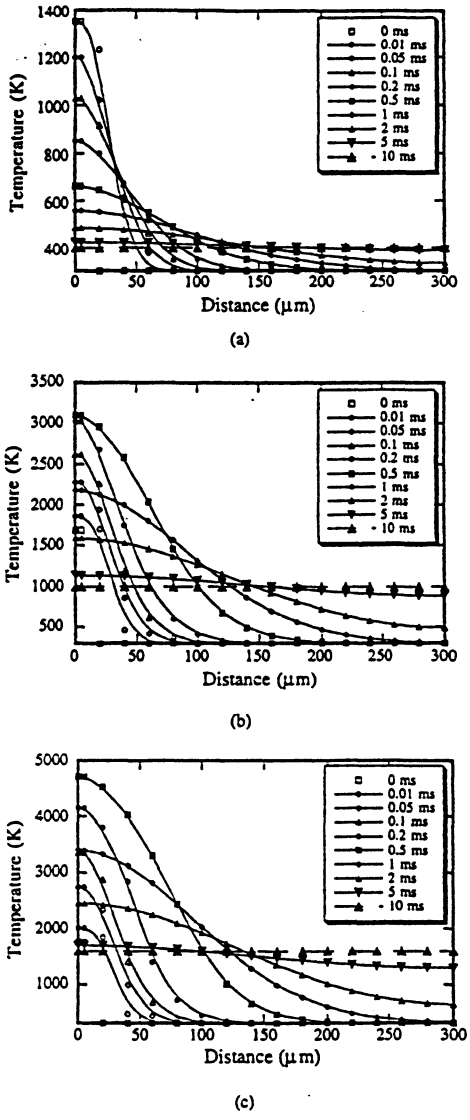

FIG. 7. Temperature distribution calculated by periodic "hot spot" model for Ti–Si mixture, $K_i=K_0$: (a) $T_s\approx1350$ K; (b) $T_s\approx1685$ K; (c) $T_s\approx1750$ K.

"equilibrium" temperature in this case, shown in Fig. 7(c), is ~1600 and ~1400 K for Fig. 8(c). Experimental results show that the entire specimen was fully reacted. Therefore, the assumption that the ignition temperature for reaction $5Ti+3Si\rightarrow Ti_5Si_3$ is close to the melting point of Si (1685 K) for conditions of the current experiments is reasonable. It should be mentioned that changing the reaction kinetics does not result in a change of heat release if reaction is completed. The tenfold increase of K inside shear band did not result in a significant change in the temperature profiles outside the shear band areas because the thickness of the shear band $\delta\ll L$ and initial conditions [Eq. (7)] provide a great difference in reaction yield inside ("hot" area) and outside the shear band ("cold" area) in the initial stage of the process even at the same K inside and outside.

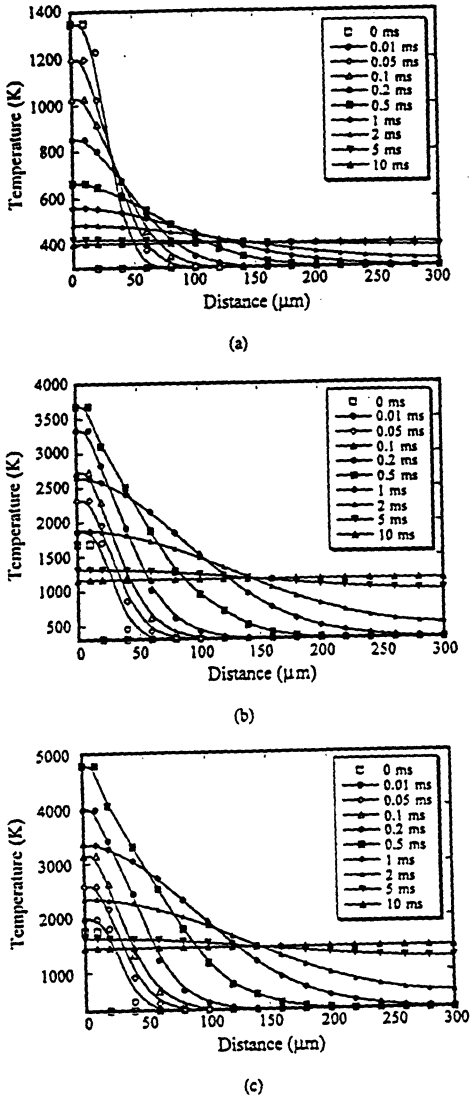

FIG. 8. Temperature distribution calculated by periodic "hot spot" model for Ti–Si mixture, $K_i = 10K_0$: (a) $T_s \sim 1350$ K; (b) $T_s \sim 1685$ K; (c) $T_s \sim 1750$ K.

Figure 9 shows the schematic diagram for the propagation of the reaction zone. Reaction is initiated inside the shear band after shear deformation work is converted into heat. The reaction front moves forward with velocity u, after the unreacted zone is heated up to 1685 K and the reaction is initiated. As time proceeds ($t_0 < t_1 < t_2$), the reaction front continues to move and more material reacts behind the reaction front. The velocity of the reaction front u, can be evaluated from Fig. 7(c). The reaction front position, x, at different times can be found from the intersections with $T = 1685$ K. Figure 10(a) shows the reaction front position, x, as a function of time. The velocity, u, is dx/dt and equal to the slope of this curve. Figure 10(b) shows the reaction front velocity as a function of time. At the beginning, the shear-band temperature is high due to the shear deformation work

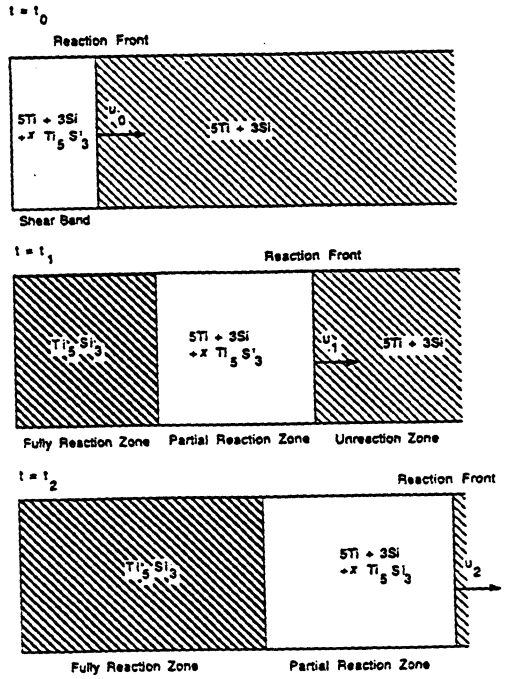

FIG. 9. Schematic representation of reaction front propagation.

and the heat released from the chemical reaction; however, outside the shear band the temperature is significantly lower ($T = 300$ K). This large temperature difference causes fast heat transfer to the unreacted zone. When the reaction is

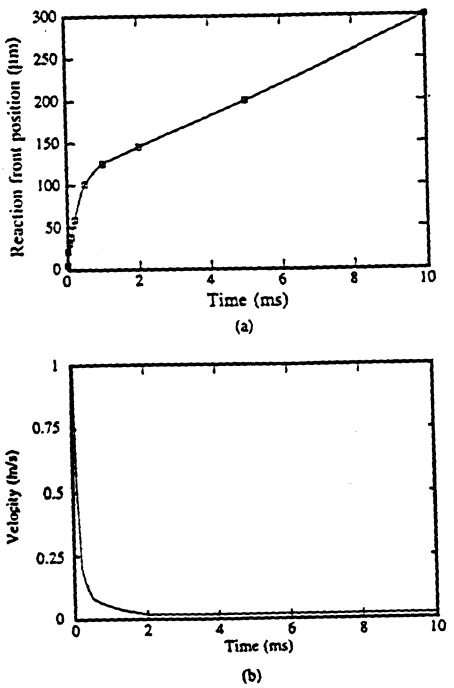

FIG. 10. (a) Position of reaction front as a function of time; (b) Velocity of reaction front vs time.

completed to form a fully reacted zone, no more energy can be released in this region. The heat released in the partial reaction zone can then be conducted to both sides, as shown in Fig. 9, and the velocity of the reaction front decreases. The velocity approaches zero with temperature decrease and an "equilibrium" state is achieved. The remaining unreacted part of the specimen will complete reaction relatively slowly in a simultaneous combustion mode if "equilibrium" temperature is close to $T_{m,Si}$.

Shear-initiated chemical reactions are also observed in the shear localization regions in Nb–Si mixtures. However, the reaction cannot propagate through the entire specimen under the same strain condition. Using the "hot spot" model, one can estimate the temperature distribution at different times. The required parameters and thermal properties for this model in the Nb–Si system are: initial temperature inside the shear band $T_s = 2000\,\text{K} \sim 2300\,\text{K}$ (corresponding to $\gamma = 20$–60); $T_0 = 300\,\text{K}$ outside the shear band; density $\rho = 4.2\,\text{g/cm}^3$; heat capacity $C_p = 540\,\text{J/kg K}$; thermal conductivity, $k = 16.8\,\text{W/m K}$; and heat release from reaction, $Q = 926\,\text{J/kg}$. The reaction kinetics are described by the same Arrhenius equation.

Since no quenched unreacted triangular region was observed in the Nb–Si system (which was used to estimate the reaction rate for the Ti–Si system by Chen *et al.*[24]), the rate constant K is unknown. The activation energy for $Nb+2Si \rightarrow NbSi_2$ was taken as 300 kJ/mol,[17] and the rate constant, K_0, equal to $\sim 10^4\ s^{-1}$.[17] Figure 11 ($K_i = K_0$) and Fig. 12 ($K_i = 10K_0$) show the results of calculation for the Nb–Si system at initial temperatures of 2000 and 2300 K. As

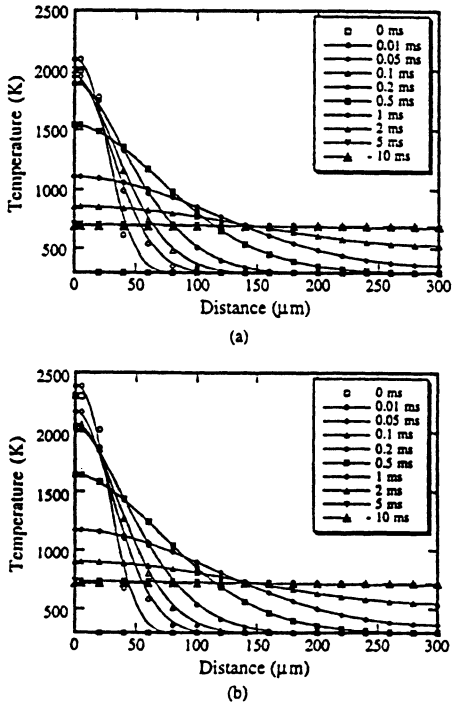

FIG. 11. Temperature distribution calculated by periodic "hot spot" model for Nb–Si mixture, $K_i = K_0$: (a) $T_s \sim 2000$ K and (b) $T_s \sim 2300$ K.

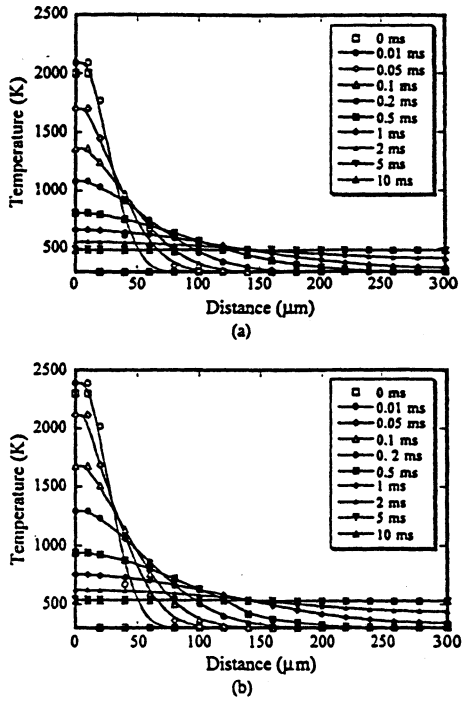

FIG. 12. Temperature distribution calculated by periodic "hot spot" model for Nb–Si mixture, $K_i = 10K_0$: (a) $T_s \sim 2000$ K and (b) $T_s \sim 2300$ K.

for the Ti–Si case, the faster reaction kinetics at both initial temperatures results in lower total reaction yield from a comparison of "equilibrium" temperatures.

In contrast with the Ti–Si system [Figs. 7(c) and 8(c)], the reaction propagates outside of the shear localization area only at distances comparable to the shear-band thickness and is rapidly quenched with "equilibrium" temperature being much lower than the Si melting temperature. This result is in accord with the experimental observations: reaction propagates from shear bands for the Ti–Si system if sufficient heat is generated, while it is localized only within the shear bands for the Nb–Si system. The enthalpy of reaction for $Nb+2Si \rightarrow NbSi_2$ ($\Delta H = -138\,\text{kJ/mol}$) is one fourth of the $5Ti+3Si \rightarrow Ti_5Si_3$ ($\Delta H = -580\,\text{kJ/mol}$) and the thermal conductivity of Nb ($k = 53.7\,\text{W/m K}$) is more than twice that of Ti ($k = 21.9\,\text{W/m K}$). Both these factors lead to the restriction of reaction propagation for the Nb–Si system.

IV. CONCLUSIONS

(1) Localized reactive shear bands were generated in Ti–Si and Nb–Si mixtures. In some experiments, reactions propagated through the entire specimen at a critical strain $\epsilon_{\text{eff}} = 0.38$ in the Ti–Si system; however, they could not take place in the Nb–Si system, under the same imposed conditions.

(2) Shear-band spacing is independent of the scale of experiment; for assemblies with mean diameters of 18 and 34 mm, the shear-band spacing is the same: $L \sim 0.6$–1 mm.

(3) Heat transfer coupled with chemical reaction calculations and with periodic boundary conditions is used to

evaluate the evolution of the temperature history from shear initiation to thermal equilibrium. The model predicts, correctly, the propagation of reaction into the intershear spaces for Ti–Si, at the experimentally observed values of shear strain in shear bands; it also predicts extinction of the reaction in the vicinity of the shear bands for the Nb–Si, in agreement with observed results.

(4) From the advance of the reaction front for the Ti–Si mixture, parallel to the shear-band interface, it is possible to estimate a reaction time by integrating the velocity (variable) over the shear-band semi-spacing. The reaction time is estimated for Ti–Si to be 10 ms and does not depend on the sample size being a function of the shear band spacing. This is in stark contrast with combustion synthesis, where the reaction time depends on the sample size in the wave propagation regime and is on the order of seconds for given sample size, and shock compression synthesis, where the reaction time can be as low as 1 μs. Thus, an intermediate reaction regime has been obtained.

(5) Reaction rate inside the shear band can be optimized for maximum reaction yield.

ACKNOWLEDGMENTS

This research was supported by the U.S. Army Research Office (Contract Nos. DAAH04-94-G-0314 and DAAH-04-95-1-0152) and by the Office of Naval Research (Contract No. N00014-94-1-1040). The authors gratefully acknowledge the support of Dr. E. Chen (ARO), J. Goldwasser (ONR), and R. Miller (ONR). Explosive experiments were carried out at the Institute of Hydrodynamics, Novosibirsk, Russia, by M. P. Bondar and Ya. L. Lukyanov, and at the Powder Metallurgy Research Institute, Minsk, Belarus, by Dr. S. Usherenko. Dr. E. Olevsky and Dr. J. C. LaSalvia provided valuable assistance with computer calculations.

[1] Z. A. Munir, Am. Ceram. Soc. Bull. 67, 345 (1988).
[2] Z. A. Munir and U. Anselmi-Tamburini, Mater. Sci. Rep. 3, 277 (1989).
[3] J. J. Moore and H. J. Feng, Prog. Mater. Sci. 39, 243 (1995).
[4] J. J. Moore and H. J. Feng, Prog. Mater. Sci. 39, 275 (1995).
[5] A. G. Merzhanov and I. P. Borovinskaya, Dokl. Akad. Nauk SSSR 204, 429 (1972).
[6] A. G. Merzhanov, in *Combustion and Plasma Synthesis of High Temperature Materials*, edited by Z. A. Munir and J. B. Holt (VCH, New York, 1990), pp. 1–53.
[7] Y. Kimura, Jpn. J. Appl. Phys. 2, 312 (1963).
[8] R. A. Graham, *Solids Under High-Pressure Shock Compression* (Springer, New York, 1993).
[9] S. S. Batsanov, *Effect of Explosions on Materials* (Springer, New York, 1994).
[10] Y. Horie and A. B. Sawaoka, *Shock Compression Chemistry of Materials* (KTK Scientific, Japan, 1993).
[11] N. N. Thadhani, Prog. Mater. Sci. 37, 117 (1993).
[12] V. F. Nesterenko, M. A. Meyers, H. C. Chen, and J. C. LaSalvia, Appl. Phys. Lett. 65, 3069 (1994).
[13] M. A. Meyers, S. S. Batsanov, S. M. Gavrilkin, H. C. Chen, J. C. LaSalvia, and F. D. S. Marquis, Mater. Sci. Eng., A 201, 150 (1995).
[14] V. F. Nesterenko, M. A. Meyers, H. C. Chen, and J. C. LaSalvia, Metall. Mater. Trans. A 26, 2511 (1995).
[15] L. H. Yu, Ph.D dissertation, New Mexico Institute of Mining and Technology, Socorro, NM, 1992, p. 204.
[16] M. W. Chase, Jr., C. A. Davies, J. R. Downey, Jr., D. J. Frurip, R. A. McDonald, and A. N. Syverud, J. Phys. Chem. Ref. Data 14, (1985), JANAF tables.
[17] M. A. Meyers, L. H. Yu, and K. S. Vecchio, Acta Metall. Mater. 42, 715 (1994).
[18] B. R. Krueger and T. Vreeland, Jr., J. Appl. Phys. 69, 710 (1991).
[19] K. S. Vecchio, L. H. Yu, and M. A. Meyers, Acta Metall. Mater. 42, 701 (1994).
[20] V. F. Nesterenko, M. P. Bondar, and I. V. Ershov, in *High-Pressure Science and Technology—1993*, edited by S. C. Schmidt, J. W. Shaner, G. A. Samara, and M. Ross (American Institute of Physics, New York, 1994), p. 1172.
[21] V. F. Nesterenko, A. N. Lazaridi, and S. A. Pershin, Fiz. Goreniya Vzryva 25, 154 (1989).
[22] A. E. H. Love, *A Treatise on the Mathematical Theory of Elasticity*, 4th ed. (Dover, New York, 1944), pp. 33–34.
[23] V. F. Nesterenko, "Controlled High-Rate-Strain Shear Bands in Inert and Reactant Porous Materials", in *SHOCK COMPRESSION OF CONDENSED MATTER-1997, Proceedings of the Conference of the American Physical Society Topical Group on Shock Compression of Condensed Matter*, 27 July–1 August 1997, Amherst, MA (APS, Ridge, NY, in press).
[24] H. C. Chen, J. C. LaSalvia, V. F. Nesterenko, and M. A. Meyers, Acta Mater. (in press).
[25] Y. Zhang and G. C. Stangle, J. Mater. Res. 8, 1703 (1993).
[26] W-C. Lee and S-L Chung, J. Am. Ceram. Soc. 80, 53 (1997).
[27] S. C. Deevi and N. N. Thadhani, Mater. Sci. Eng., A 192/193, 604 (1995).